J. theor. Biol. (1995) **174**, 371–380

Ferroelectric Behavior in Microtubule Dipole Lattices: Implications for Information Processing, Signaling and Assembly/Disassembly

J. A. TUSZYŃSKI†, S. HAMEROFF‡, M. V. SATARIĆ§, B. TRPISOVÁ† AND M. L. A. NIP†

† *Department of Physics, University of Alberta, Edmonton, Alberta, T6G 231, Canada,*
‡ *Department of Anesthesiology, University of Arizona, Tucson, Arizona, 85724, U.S.A.*
and § Faculty of Technical Sciences, 21 000 Novi Sad, Serbia

(*Received on 26 May 1993, Accepted in revised form on 3 January 1995*)

Cytoskeletal microtubules structurally organize interiors of living eukaryotic cells. As polymers of subunit proteins ("tubulin"), which are each dipoles, microtubules are thus lattices of oriented dipoles. In general, three types of arrangements of dipoles in lattices may occur: (i) random, (ii) ferroelectric (parallel-aligned) and (iii) an intermediate weakly ferroelectric phase, which is length-dependent. Because of involvement in dynamical cell activities (movement, growth, mitosis, differentiation, etc.), models of microtubule signaling and information processing have been proposed. In these, tubulin units are assumed to represent informational "bit states" and to be coupled to intra-tubulin dipoles. In the present paper, we consider microtubules as lattice arrays of coupled local dipole states that interact with their immediate neighbors. Depending on the values of assumed model parameters, the system may exhibit "frustration": conflict in satisfying all dipole couplings. Such systems have properties suitable for efficient information processing and computation. By slightly altering temperature and external field (both within physiological conditions), microtubule dipole lattices may assume a ferroelectric phase with long-range order and alignment with capabilities to propagate kink-like excitations. The ferroelectric phase appears to be optimal for microtubule signaling and assembly/disassembly. Microtubules may organize cell activities by operating in different modes suitable for information processing and computation (intermediate phase) or signaling and assembly/disassembly (ferroelectric phase).

1. Introduction

Interiors of living cells are structurally and dynamically organized by networks of protein polymers called the cytoskeleton. Of these filamentous structures which include actin and intermediate filaments, microtubules (MTs) are the best characterized and appear to be the most fundamental (Dustin, 1984). MTs are hollow cylinders 25 nanometers (nm) in diameter whose lengths may span macroscopic dimensions. MTs are assemblies of 13 longitudinal protofilaments, each of which is a series of subunit proteins known as tubulin (Fig. 1). Each tubulin subunit is a polar, 8 nm-long dimer which consists of two slightly different 4 nm-long monomers, each with a molecular weight of 55 kDa. These two constituent parts are referred to as α and β tubulin. Each dimer has a net mobile electronegative charge due to an abundance of acidic amino acids, and binds 18 calcium ions. The net negative mobile charge is localized predominantly towards the α monomer so that each tubulin dimer bears an oriented dipole. Thus, MTs are an example of an electret substance, i.e. an assembly of oriented dipoles. In this paper we investigate the types of spatial arrangements of these dipoles in detail and their implications on MT behavior.

Conformational states of tubulin dimers present within MTs have been suggested to be coupled to charge or dipolar states, thereby allowing for cooperative interactions with neighboring tubulin dimer sites (Hameroff & Watt, 1982; Hameroff, 1987;

0022-5193/95/120371 + 10 $08.00/0

Rasmussen *et al.*, 1990). This coupling would also lead to the presence of piezoelectric properties which are very common in ferroelectrics which, in turn, could prove very important in MT signaling, communication and assembly/disassembly behavior (Athenstaedt, 1974; Margulis *et al.*, 1978).

MT associated proteins (MAPs) which may be structural, contractile or enzymatic are attached to MTs at specific tubulin dimer sites and can link MTs with other MTs, other parallel arrayed cytoskeletal elements, membranes and organelles to form networks and scaffolding within living cells. MAP attachment sites may be irregular, or can describe various helical patterns on MT surface lattices (Burns, 1978; Kim *et al.*, 1986). The focal point of the cytoskeleton is the centriole, a pair of cylindrical assemblies of nine MT triplets oriented perpendicular to each other. Centrioles organize the array of cytoplasmic MTs during interphase, duplicate at mitosis to nucleate the two poles of the mitotic spindle and establish orientation and architecture for the next generation of cells.

Genes for α and β tubulin are complex, multi-gene families that give rise to varying tubulin isozymes. During evolution, some tubulins have been highly conserved for basic cell functions; however, extensive MT heterogeneity exists in complex cells due to genetic diversity, expression, post-translational modifications, MAPs and assembly patterns. For example, two-dimensional gel electrophoresis has shown 17 different varieties of β tubulin exist in mammalian brain MTs, whereas fewer exist in other tissues (Lee *et al.*, 1986). Tubulin structure may also be altered by "post-translational" modification: enzymatic alteration (usually addition or removal of amino acids such as glycosylation or detyrosination) triggered by intracellular events including second messenger activities.

MT self-assembly and disassembly are dynamic, complex processes whose states depend on various factors including temperature and calcium ion concentration. Oriented by centrioles, MT polymerization determines the architecture and form of cells which can quickly change by MT depolymerization and reassembly in another direction. GTP, an energy-providing analog of ATP, binds to free, unpolymerized tubulin; GTP-tubulins then self assemble to form MTs in an entropy driven process. Within assembled MTs, GTP hydrolyzes to GDP, imparting energy into the MT lattice via tubulin conformational changes. MTs whose ends are comprised of GTP-tubulin are stable and will continue to grow. MTs whose ends are comprised of GDP-tubulin are unstable and will depolymerize rapidly. As GTP is hydrolyzed to GDP within MT, GDP-tubulin is exposed at MT ends and, unless stabilized by MAPs, centrioles or other structures, MTs rapidly disassemble. Free GDP-tubulin is reconverted to GTP-tubulin which becomes available for reassembly. *In vitro*, this "dynamic instability" (Kirschner & Michison, 1986; Hotani *et al.*, 1992) results in erratic alterations between growing and shrinking phases; *in vivo* "selectionist" activity occurs in which MT networks can adaptively probe or retreat in cellular appendages including axonal and dendritic growth cones and developing synapses (e.g. Reinsch *et al.*, 1991; Sabry *et al.*, 1991). Recent works have shown that MT spatial structures or patterns may form under the maintenance of a sustained energy source (GTP hydrolysis), suggesting that MTs may be dissipative structures (Tabony & Job, 1990, 1992).

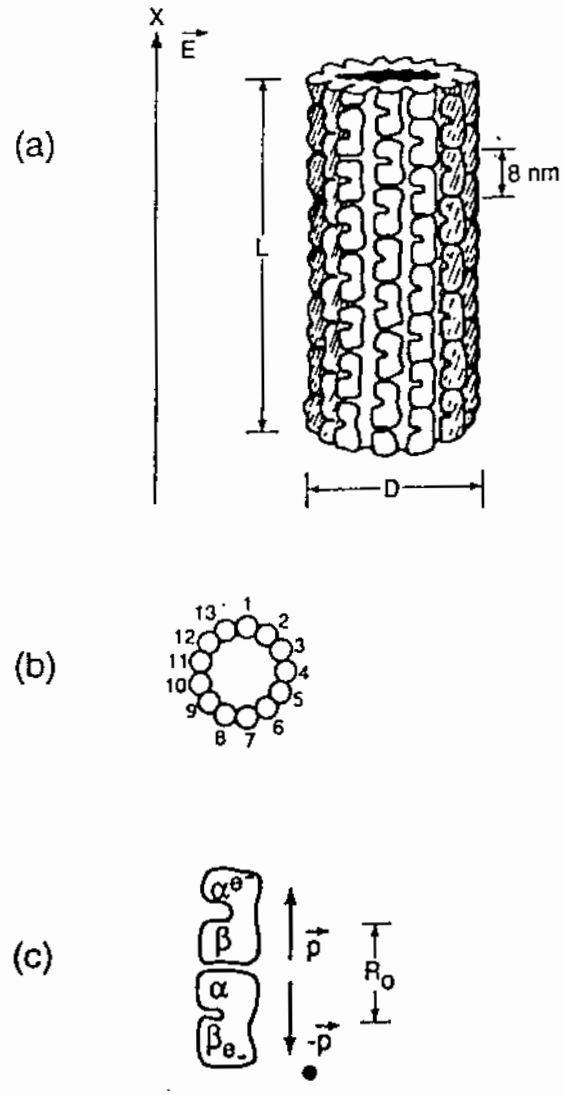

FIG. 1. An illustration of the microtubular arrangement.

Some evidence links the cytoskeleton with information processing and cognitive function. For example, Mileusnic *et al.* (1980) correlated production of MT subunit protein ("tubulin") and MT activities with peak learning, memory and experience in baby chick brains. Cronley-Dillon *et al.* (1974) showed that when baby rats begin their critical learning phase for the visual system (when they first open their eyes), neurons in the visual cortex begin producing vast quantities of tubulin. Tubulin production is drastically reduced when the critical learning phase is over (when the rats are 35 days old). Moshkov *et al.* (1992) showed structural and chemical changes in goldfish brain neuronal cytoskeleton following sensory stimulation. In gerbils exposed to cerebral ischemia, Kudo *et al.* (1990) correlated the amount of reduction in dendritic MAP-2 with the degree of cognitive impairment. Bensimon & Chernat (1991) found that selective destruction of brain MTs by the drug colchicine caused cognitive defects in learning and memory which mimic the clinical symptoms of Alzheimer's disease, in which the cytoskeleton becomes entangled. Geerts *et al.* (1992) showed that sabeluzole, a memory-enhancing drug, increases fast axoplasmic transport. Matsuyama & Jarvik (1989) have proposed that Alzheimer's is a disease of MTs and MAPs. In specific hippocampal regions of the brains of schizophrenic patients, Arnold *et al.* (1991) found distorted neuronal architecture due to a lack of two MAPs (MAP-2 and MAP-5).

Models of learning in mammalian NMDA (n-methyl-d-aspartate) hippocampal neurons (i.e. long-term potentiation—LTP) involve pre- and post-synaptic enhancement of synaptic function. Silva *et al.* (1992) have shown calcium-calmodulin kinase to be essential for LTP. Aszodi *et al.* (1991) have demonstrated protein kinase A to be involved in learning. Halpain & Greengard (1990) have shown that post-synaptic activation of NMDA receptors induces rapid dephosphorylation of dendrite-specific MAP-2. Aoki & Siekevitz (1988) linked learning to protein kinase C mediated MAP-2 phosphorylation/ dephosphorylation, and Theurkauf & Vallee (1983) demonstrated that MAP-2 phosphorylation/ dephosphorylation consumed a huge proportion of brain biochemical energy. Bigot & Hunt (1990) showed that NMDA and other excitatory amino acid neurotransmitters caused redistribution of intraneuronal MAPs, and Wang & Rasenick (1991) have shown that G proteins directly link with MTs. Surridge & Burns (1992) demonstrated that the lipid second messenger phosphatidylinositol binds specifically to MAP-2, a coupling which may "constitute a link by which extracellular factors influence the microtubule cytoskeleton". Kwak & Matus (1988) showed that denervation caused long-lasting changes in MAP distribution, and Desmond & Levy (1988) showed that LTP involved cytoskeletal-mediated shape changes in dendritic spines. Lynch & Baudry (1987) have proposed that proteolytic digestion of the sub-synaptic cytoskeleton, followed by its structural reorganization, correlate with learning, and Friedrich (1990) has formalized a learning model of synaptic cytoskeletal restructuring. Synaptic regulation, both in learning and steady state, also depends on material (enzymes, receptors, neurotransmitters, etc.) synthesized in the cell body and transported along axons and dendrites by contractile MAPs attached to MT ("axoplasmic transport"). Similar mechanisms involving actin, synapsin and other cytoskeletal polymers are involved in neurotransmitter release.

Further suggestion for cytoskeletal computation and/or information storage stems from the spatial distribution of discrete sites (or states) in the cytoskeleton. For example, tubulin subunits in closely arrayed MTs have a density of about 10^{17} cm^{-3}, which is very close to the theoretical limit for charge separation (Gutmann, 1986). Thus cytoskeletal polymers have maximal density for information representation by charge, and the capacity for dynamically coupling that information to mechanical and chemical events via cooperative dipole states.

Previous papers have modeled signaling and information processing in MTs based on coherent phonons, solitons and cellular automata based on dipole coupled conformational states of tubulin.

In this paper we address the question of how some functions of MTs (i.e. assembly/disassembly and proposed signaling and information processing) may be related to the ground state properties of the lattice of dipoles. In general, three kinds of geometrical arrangements of dipoles are found: (i) random where no order in the dipole arrangements exists, (ii) ferroelectric (long-range parallel-aligned order) and (iii) intermediate, weakly ferroelectric where short range order is present. Each of these arrangements may exist under different conditions of temperature, electric field and MT length, and a single MT may switch among the different arrangements. The long-range ordered ferroelectric state appears most suitable for assembly/disassembly and signaling processes while the short-range ordered weakly ferroelectric state is well suited for information processing. In the next two sections we discuss these properties in detail.

2. The Dipolar Lattice and its Phases

Our basic premise physically views the entire MT as a regular array of coupled local dipole states

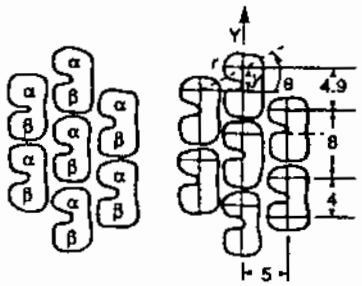

FIG. 2. A tubulin dimer and its nearest neighbors.

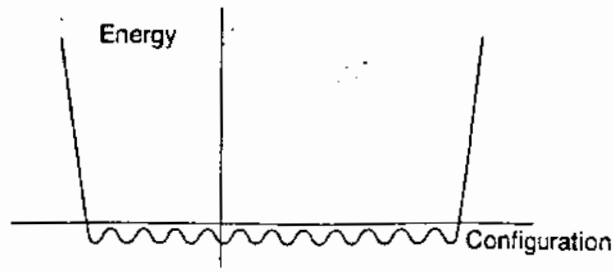

FIG. 4. A schematic representation of the energy dependence on conformational states.

which interact with their immediate neighbors. Although tubulin undergoes conformational changes (e.g. Melki *et al.*, 1989), we adopt a simplified view in which elastic degrees of freedom are not explicitly included in the description. We will return to this question in the Discussion.

The starting point in the analysis is to adopt a hexagonal lattice structure with the dimensions and orientations observed by X-ray diffraction of MTs and shown in Fig. 2. Each lattice site is assumed to possess a dipole moment $p = Q \cdot d$ where $Q = 2e$ and $d \cong 4$ nm whose projections on the vertical axis can only be $+p$ or $-p$. The interaction energy between two neighboring lattice sites is

$$H_{ij} = \frac{1}{4\pi\epsilon\epsilon_0} \frac{3\cos^2\theta - 1}{r_{ij}^3} p^2, \tag{1}$$

where ϵ_0 is the vacuum permittivity and r_{ij} is the distance between sites i and j. The angle θ is between the dipole axis and the direction between the two dipoles. Figure 3 illustrates the situation resulting from our calculations.

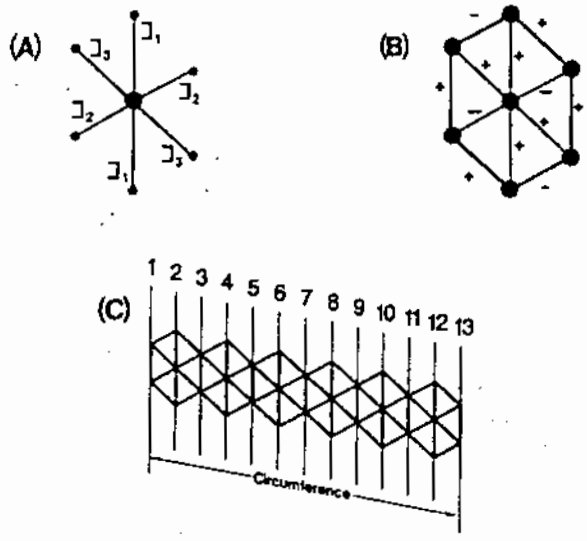

FIG. 3. Exchange constants (a) and their signs (b) within a unit hexagonal cell. (c) A band of hexagons spanning the circumference of a microtubule.

In Fig. 3(b) the signs "+" and "−" refer to dipole–dipole interactions that prefer either a parallel or antiparallel arrangements of dipole moments, respectively. Below, we present the numerical results for the constants J_1, J_2, J_3 and the corresponding angles.

$$J_1 = 5.77 \times 10^{-21}\ \text{J} \quad \theta_1 = 0°$$

$$J_2 = -0.71 \times 10^{-21}\ \text{J} \quad \theta_2 = 58.2°$$

$$J_3 = 3.40 \times 10^{-21}\ \text{J} \quad \theta_3 = 45.6°$$

We can, therefore, map this situation as an anisotropic two-dimensional Ising model on a triangular lattice so that the effective Hamiltonian is

$$H = \underset{\langle nn \rangle}{-\Sigma} J_{ij} S_i^z S_j^z, \tag{2}$$

and the effective spin variable $S_i^z = \pm 1$ denotes the dipole's projection on the vertical axis. The exchange constants J_{ij} take the values J_1, J_2, J_3 depending on the choice of dipole pairs.

What, therefore, appears in Fig. 3(b) is that the system exhibits a certain amount of *frustration* (Suzuki, 1977) in its ground state. This means that for a closed path around the 13 protofilaments of the microtubule, it is impossible to satisfy all bond requirements since there is an odd number of antiparallel bonds. Note that no frustration exists in the direction along the MT axis giving the overall ferroelectric character to the lattice. It will also be seen how this is manifested through size dependence of net polarization.

Small potential barriers separating the various equivalent arrangements of spins (see Fig. 4) play another useful role. Relaxation times are very long for the various accessible states giving them long-term stability. Some other properties of this intermediate, weakly ferroelectric phase are: (i) absence of long-range order between spin sites and (ii) the presence of short-range correlations. This means that the system is very "soft" energetically, permitting a number of spin arrangements which are relatively

stable. However, there is no tendency towards the formation of large correlated spin clusters. This intermediate phase also allows easy formation of local ordered states, each of which carries an information content and is long-lived, i.e. relatively stable over time. On the other hand, it is not difficult to switch from one local state to another through various physical means by overcoming local potential barriers. Furthermore, a complete phase transformation can be achieved by:

(i) an application of an electric field along the axis. We estimate that intracellular fields on the order of $10^4\ \mathrm{Vm}^{-1}$ are sufficient to switch an MT from an intermediate state to a ferroelectric state (F). (Note that fields up to $10^7\ \mathrm{Vm}^{-1}$ are known to exist across cell membranes).

(ii) Raising the temperature above the ferroelectric transition temperature will drive the system to a disordered (paraelectric) phase.

We mentioned above that another ordered phase is favored when a moderate external field is applied (or indeed when the temperature is lowered further). This phase, called a ferroelectric phase, is characterized by long-range order manifested by an alignment of spin directions along the axis. This is shown in Fig. 5. Obviously, from the point of view of optimal information content, this is *not* a very useful phase. However, the ferroelectric phase can play a major role in signaling and the assembly/disassembly processes. This will be discussed at length in the next Section. Before we discuss this aspect, we investigate its general properties. The ferroelectric phase can also be destabilized by temperature when T exceeds T_c. To obtain a crude estimate of T_c we approximated the MT by an infinite triangular lattice with the exchange constants J_1, J_2 and J_3 given above and used the formula (Domb, 1960).

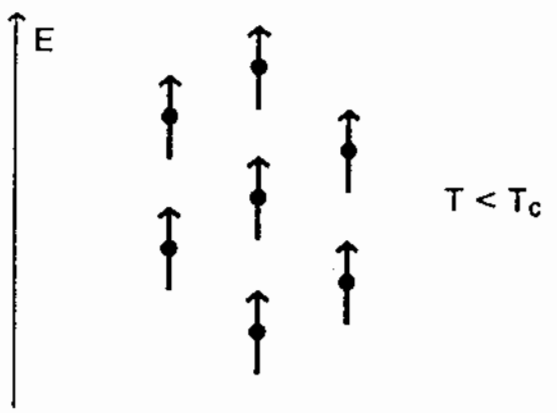

FIG. 5. The dipole orientations in the ferroelectric state.

$$\sinh\left(\frac{2J_1}{K_BT_C}\right)\sinh\left(\frac{2J_2}{K_BT_C}\right) + \sinh\left(\frac{2J_1}{K_BT_C}\right)\sinh\left(\frac{2J_3}{K_BT_C}\right) + \sinh\left(\frac{2J_2}{K_BT_C}\right)\sinh\left(\frac{2J_3}{K_BT_C}\right) = 1. \qquad (3)$$

The result we obtained using the above crude estimate for an infinitely long lattice is $T_c \cong 402\ K$ *for the charge of* $q = 2e$, the permittivity $\epsilon = 10$ and the dipole displacement $d = 4$ nm. On the other hand, taking $q = 1e$, $\epsilon = 5$ and $d = 4$ nm yields $T_c = 201$ K. These two very rough estimates of T_c indicate nevertheless that it is feasible to expect an interesting phase behavior in the physiological temperature range around 300 K for a specific choice of model parameters. In addition, it is well known that the size of a lattice affects T_c greatly. In general, for size N, $T_c(N)$ is related to that for an infinite lattice $T_c(\infty)$ through (Binder *et al.*, 1985):

$$T_c(N) = T_c(\infty) - \alpha N^{-1/\gamma}, \qquad (4)$$

where α is an approximate proportionality coefficient and γ is the correlation length exponent (typically close to 1/2). Thus, for a finite-size lattice, the transition temperature is expected to be less than that for an infinite lattice. In other words, dipole ordering is more likely to occur when a critical size of the MT is achieved. In addition, other important factors may affect the value of T_c and thus provide sensitive control mechanisms. Through a coupling to the elastic degrees of freedom (conformational change), the value of T_c may be shifted. The dielectric constant ϵ may be altered by the presence of water molecules surrounding an MT structure. This would decrease the value of T_c and introduce disorder. Small changes in the angles between the dimer dipoles may remove the frustration mechanism effectively preventing the onset of the intermediate phase. Changes in the opposite direction can enhance frustration favoring the intermediate phase over the F phase and effectively switching from the growth mode of operation to an information processing behavior. Thus symmetry transitions or mechanical forces may effect switching between phases.

Once in the ferroelectric phase, the system is also very sensitive to the frequency of electromagnetic oscillations. It is known that in organic ferroelectric materials a resonant frequency exists W_0 which is inversely proportional to the length, stiffness constant

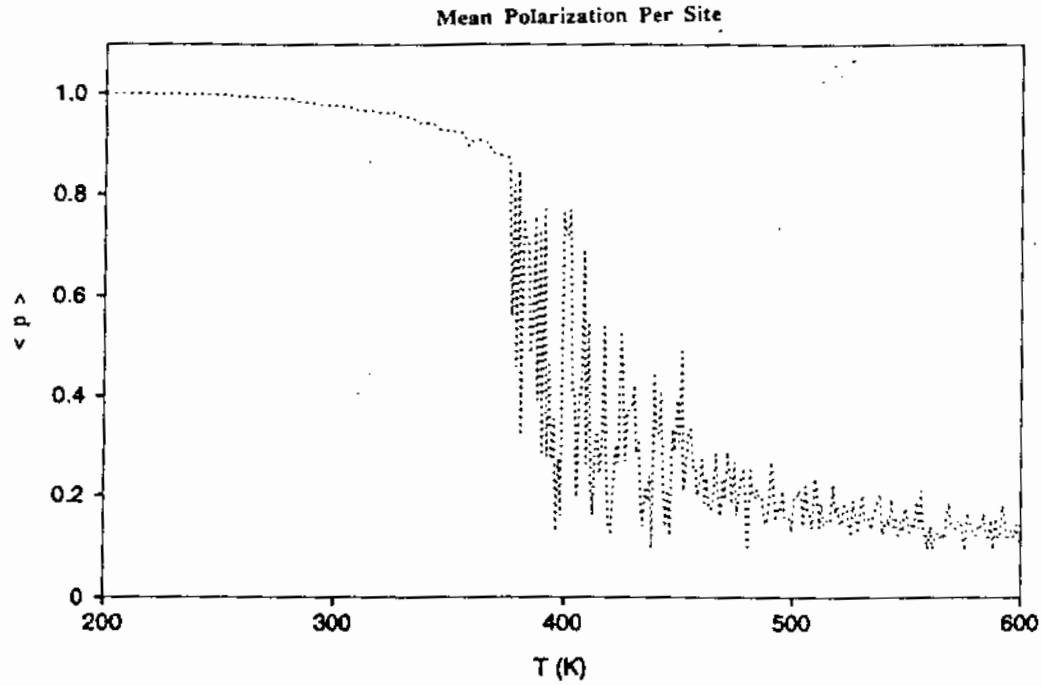

FIG. 6. A plot of the mean polarization per site for a triangular lattice whose size is 13 × 26.

and the square root of the density (Matthias, 1973). Extrapolating the data given by Matthias (1973), one finds for microtubules a resonant frequency range exceeding 10^8 Hz and thus being rather close to the microwave range predicted by Fröhlich (1980) to play a major role in living cells.

In Figs 6 and 7 we have shown the results of our Monte Carlo computations intended to reveal the size dependence of the phase behavior discussed above. Figure 6 is a plot of the mean polarization per site when the microtubule is composed of only 26 layers (i.e. it is a 13 × 26 lattice). It is clear that three distinct ranges exist: (i) the low-temperature ferroelectric range, (ii) the intermediate weakly ordered phase range and (iii) the high-temperature paraelectric range. Figure 7 illustrates the same dependence for a microtubule with 5000 layers (i.e. it is a 13 × 5000 lattice). We conclude that the intermediate weakly ferroelectric phase all but disappeared.

To summarize, in this section we have argued that two ordered phases are likely to govern the behavior of dipole moments in an MT. A ferroelectric phase is characterized by long-range order and has many characteristics useful in energy transfer properties discussed in the next section. An intermediate weakly ordered phase exhibits short-range order but has a multitude of equivalent, long-lived dipolar states. It appears that in the latter phase the system can explore a large subset of the phase space at a low energetical cost unlike in the ferroelectric phase. Having unhindered access to a multitude of conformational states indicates easy transitions from one configuration to another at little or no energy cost. A number of control mechanisms are possible which allow switching from one phase to the other and hence from one mode of operation to the other.

3. Ferroelectricity, Signaling and Assembly/Disassembly

It is well known that ferroelectrics are one of the few types of materials whose description is most adequately provided in terms of mean field models (Kretschmer & Binder, 1979). A typical approach is to postulate a double-well quartic on-site potential $V(S_n)$ that gives the overall effect of the environment on a selected dipole site n. Thus,

$$V(S_n) = -\tfrac{1}{2}AS_n^2 + \tfrac{1}{4}BS_n^4, \qquad (5)$$

where S_n is the effective spin variable at site n and the coefficients A and B are model-dependent. It will be subsequently assumed that over long distances the variable S_n changes very gradually and can be treated as a continuous variable.

In the F phase, the MT cylinder taken as a whole represents a giant dipole. When the cross-section of an MT is viewed using electron microscopy, the outer surfaces of an MT are surrounded by a "clear zone" of several nm which apparently represents the oriented molecules of cytoplasmic water and enzymes (Steb-

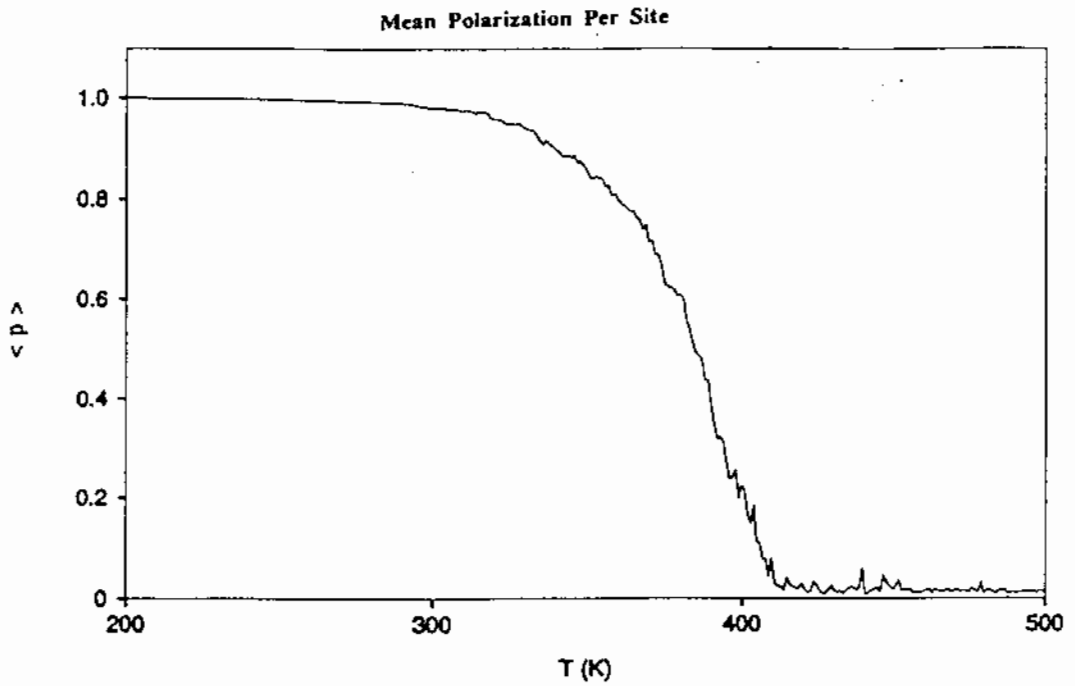

FIG. 7. A plot of the mean polarization per site for a triangular lattice whose size is 13 × 5000.

bings & Hunt, 1982). This could be explained by the presence of an electric field produced by an MT. Therefore, we assume that together with the polarized water surrounding it, an MT generates a nearly uniform intrinsic electric field parallel to its axis (see Fig. 1). Consequently, the additional potential energy due to this electric field and associated with each dipole is

$$V_{el} = -CS_n, \quad C = qE, \tag{6}$$

where q denotes the effective charge of a single dimer and E is the magnitude of the intrinsic electric field. Within this picture, the model Hamiltonian for the dipole moments of a microtubule can be written as

$$H = \sum_{n=1}^{n} \left[\frac{1}{2} M \left(\frac{dS_n}{dt} \right)^2 + \frac{1}{2} K (S_{n+1} - S_n)^2 - \frac{A}{2} S_n^2 + \frac{B}{4} S_n^4 - CS_n \right]. \tag{7}$$

The first term above represents the kinetic energy associated with the longitudinal displacements of constituent dimers each of which has mass M. The second term arises from the restoring strain forces between adjacent dimers in the protofilament. If the stiffness parameter K is sufficiently large, then it is expected that large-amplitude long-wavelength excitations of the displacement field will be formed manifested by a slowly varying modulation of S_n along the MT axis.

In order to derive a realistic equation of motion for this system, the viscosity of the solvent is indispensable and the associated damping force must be introduced. Assuming for simplicity that the solvent is made up of only water molecules we may infer that water will provide a viscous medium that will damp out vibrations of dimer dipoles. This can be taken into account by adding the viscous force to the equation of motion with

$$F = -\gamma \frac{dS_n}{dt},$$

where γ is the damping coefficient.

Based on our assumption that the dipolar oscillations of dimers within an MT form a system that can be classified as displacive ferrodistortive, we can use the continuum approximation to obtain the corresponding equation of motion as

$$M \frac{d^2S}{dt^2} - KR_0^2 \frac{d^2S}{dx^2} - AS + BS^3 + \gamma \frac{dS}{dt} - qE = 0. \tag{8}$$

Note that the x-coordinate is along the protofilament axis. Moreover, for longitudinal sound waves the dispersion relation

$$\omega = \sqrt{K/M}$$

can be used to identify the sound velocity with

$$V_0^2 = \omega R_0 = \sqrt{K/M}\, R_0.$$

We now seek solutions of eqn (7) in the traveling-wave form where the moving coordinate ξ is given by

$$\xi = \left[\frac{|A|}{M(V_0^2 - V^2)}\right]^{1/2}(x - Vt) = \alpha(x - Vt), \quad (9)$$

with V denoting the propagation velocity and the coefficient α is, of course,

$$\alpha = \left[\frac{|A|}{M(V_0^2 - V^2)}\right]^{1/2}$$

Consequently, eqn (8) is reduced to the ordinary differential equation below

$$M\alpha^2(V^2 - V_0^2)S'' - \gamma\alpha VS' - AS + BS^3 - qE = 0, \quad (10)$$

where $S' \equiv dS/d\xi$. This is an equation for an anharmonic oscillator with linear friction.

For the sake of convenience we now introduce a normalized displacement field as:

$$\Psi(\xi) = S(\xi)/S_0$$

where the normalizing coefficient

$$S_0 = \sqrt{|A|/B}$$

corresponds to the minimum of the double well potential in eqn (5).

It has been shown by Collins *et al.* (1979) that eqn (10) has a unique bounded solution which is given by the formula (and illustrated graphically in Fig. 8)

$$\Psi(\xi) = a + \frac{b - a}{1 + \exp(\beta\xi)}, \quad (11)$$

where

$$\beta = (b - a)/\sqrt{2}$$

and the parameters a, b and d satisfy the cubic equation

$$(\Psi - a)(\Psi - b)(\Psi - d) = \Psi^3 - \Psi - \sigma, \quad (12)$$

where

$$\sigma = q\sqrt{B}|A|^{-3/2}E.$$

Formula (11) describes a kink-like excitation (KLE) which takes the form of a domain wall separating two distinct ferroelectric domains.

It is also important to note that the above kink-like soliton propagates along the protofilament with a fixed velocity

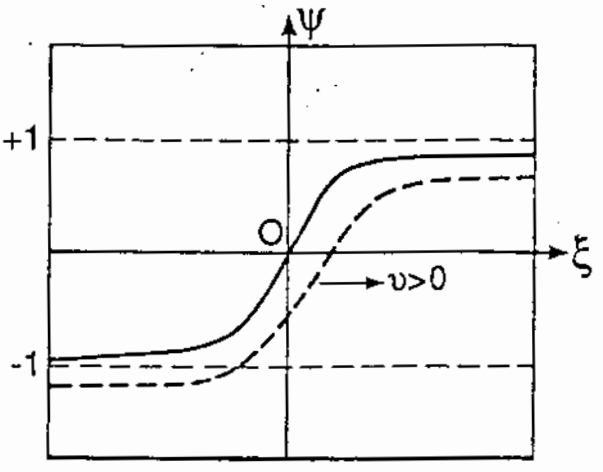

FIG. 8. The kink-like profile to the solution $\Psi(\xi)$ of eqn (11).

$$V = V_0/\left[1 + \frac{2\gamma^2}{9d^2MV_0^2}\right]^{1/2}, \quad (13)$$

which is *less* than the sound velocity V_0 and decreases with an increase of the friction coefficient γ. It is clear that V depends on the magnitude of the electric field E through the parameter d.

For T well below T_c, V can be approximated by a linear relationship with E

$$V \approx \frac{3V_0}{\gamma|A|}\sqrt{\frac{MB}{2}}\, qE, \quad (14)$$

where the coefficient of proportionality is called mobility and will be denoted by μ. Using simple arguments from fluid dynamics, μ can be estimated numerically as

$$\mu \approx 2 \times 10^{-5}\ \mathrm{m^2\ V^{-1}\ sec^{-1}}$$

Thus, for $E = 10^5\ \mathrm{V\ m^{-1}}$ we obtain $V \cong 2\ \mathrm{m\ sec^{-1}}$ which can increase to $10^2\ \mathrm{m\ sec^{-1}}$ close to the MTs ends where E increases dramatically.

Assuming a smooth journey from one end of the protofilament to the other we estimate the average time of propagation $\bar{T}$ for a single KLE to be

$$\bar{T} = \frac{L}{V} \approx 5 \times 10^{-7}\ \mathrm{sec}$$

A recent paper (Chou *et al.*, 1994) also pointed to the possible role of solitary waves in the dynamics of microtubules.

To summarize, we showed that a unique kink-like excitation exists in the ferroelectric phase which

may propagate along an MT with a velocity that is proportional to the electric field E. KLEs in stable microtubules may constitute signals transducing membrane events via second messengers to other cell regions. Energy for such KLEs may come from GTP hydrolysis or phosphorylation via MAPs. In neurons, KLEs in microtubules may signal error information retrograde (i.e. from axon to dendrite) which would be useful in synaptic regulation and learning as in artificial neural network "back-propagation". In unstable MTs (i.e. whose ends are not stabilized by MAPs or other structures), KLEs can explain the fact that growth rates are different at the two ends of an MT. To this end, we assume that KLE formation is mainly due to the hydrolysis of GTP into GDP so that one act of hydrolysis corresponds to conformational change resulting in the formation of a single KLE. However, a KLE is preferentially oriented towards the direction of the intrinsic electric field. The propagation of a KLE will then distribute the energy of hydrolysis at the preferred end of an MT. This energy may then be used to detach dimers from the MT. This picture is in accordance with a hypothesis put forward by Kirschner & Mitchison (1986) who stated that on-rate (growth) is limited in principle only by the rate of diffusion of the monomer subunits into MT polymers (i.e. by the concentration of the constituent monomers in solution). On the other hand, the off-rate (depolymerization) can be extremely rapid and the net amount of MT polymer formed can be regulated independently by the hydrolysis of GTP.

It is reasonable to expect that at the onset of the MT assembly process, when MTs are very short, the formation of KLEs is very unlikely (or even impossible), since for a short chain the displacement field gradient required would be very high and the associated energy to form it prohibitively large. However, when the length of an MT reaches a threshold value, kink propagation could become a real possibility. Excitation of kinks being related to GTP hydrolysis would become dependent on the GTP concentration. As MTs become longer, KLE propagation accelerates leading to a disassembly at the "-" end. KLE propagation in stable MTs would depend on MAP phosphorylation or cytoplasmic kinase activity triggered by membrane events and second messengers.

4. Summary

We have argued in this paper that the spatial arrangement of dipole moments of a microtubule is crucial to its functioning as a dynamic system. Due to the presence of frustration in the dipole–dipole interactions, an intermediate weakly ferroelectric phase is predicted to arise at low enough temperatures and electric fields as well as for sufficiently short microtubules. Its attractiveness lies in maximal computational capabilities offered by a highly degenerate ground state and by long relaxation times giving relative stability to short-range correlated dipole patterns. Each pattern can be seen as containing binary information. This phase strongly resembles the well-known spin glass phenomenon which has received much attention in frustrated spin systems such as random-anisotropy magnets. Recently, spin-glass models have been applied in connection with biological systems (Stein, 1992).

The other possible ordered state is a ferroelectric phase with an almost perfect alignment of dipole movement along the protofilament axis. It is characterized by long-range order and hence its usefulness for information processing is dubious. However, it eagerly supports the formation of domain walls between the two stable orientations of dipole movements. The application of an external electric field preferentially directs kink-like excitations towards the properly aligned end. These kink-like excitations may be utilized as signaling mechanisms or causing disassembly due to energy release.

We have discussed the various possible control mechanisms (temperature, electric field, mechanical distortion) that could select the MT operating modes among information processing, weakly ordered and signaling and assembly/disassembly (ferroelectric) types.

This research was supported by NSERC (Canada), the Alexander von Humboldt Foundation and (SRH) NSF Grant No. DMS-9114503. The authors are indebted to MIDIT, Danish Technical University for summer support in 1994.

REFERENCES

Aoki, C. & Siekevitz, P. (1988). *Sci. Am.* **259**(6), 56–64.
Arnold, S. E., Lee, V. M. Y., Gur, R. E. & Trojanowski, J. Q. (1991). *Proc. natn. Acad. Sci. U.S.A.* **88**, 10850–10854.
Athenstaedt, H. (1974). *Ann. N.Y. Acad. Sci.* **238**, 68.
Barnett, M. (1987). In: *Proceedings of the 3rd Molecular Electronic Device Conference* (Carter, F., ed.) Washington, DC: Naval Research Laboratory.
Bensimon, G. & Chernat, R. (1991). *Pharmacol. Biochem. Behav.* **38**: 141–145.
Bigot, D. & Hunt, S. P. (1990). *Neurosci. Lett.* **111**: 275–280.
Binder, K., Nauenberg, M., Privman, V. & Young, A. P. (1985). *Phys. Rev. B* **31**, 1498.
Burns, R. B. (1978). *J. Ultrastruct. Res.* **65**, 73–82.
Chou, K. C., Zhang, C. T. & Maggiora, G. M. (1994). *Biopolymers* **34**, 143–153.
Collins, M. A., Blumen, A., Currie, J. F. & Ross, J. (1979). *Phys. Rev. B* **19**, 3630.
Cronly-Dillon, J., Carden, D. & Birks, C. (1974). *J. expl Biol.* **61**, 443–454.

DESMOND, N. L. & LEVY, W. B. (1988). *Long-Term Potentiation: From Biophysics to Behavior* (Landfield, P. W. & Deadwyler, S. A. eds) New York: Liss.
DOMB, D. (1960). *Phil. Ma Suppl.* **9**, 35.
DUSTIN, P. (1984). *Microtubules*. Berlin: Springer.
FRIEDRICH, P. (1990). *Neurosci.* **35**, 1–7.
FRÖHLICH, H. (1980). *Adv. Electr. Electr. Phys.* **53**, 85.
GEERTS, H., NUYDENS, R., NUYENS, R., CORNELISSEN, F., DE BRABANDER, M., PAUWELS, P., JANSSEN, P. A. J., SONG, Y. H. & MANDELKOW, E. M. (1992). *Expl. Neur.* **117**, 36–43.
GUTMANN, F. (1986). *Modern Bioelectrochemistry* (Gutmann, F. & Keyzer, H., eds) pp. 177–197. New York: Plenum Press.
HALPAIN, S. & GREENGARD, P. (1990). *Neuron* **5**, 237–246.
HAMEROFF, S. (1987). *Ultimate Computing*. Amsterdam: Elsevier North-Holland.
HAMEROFF, S. R., DAYHOFF, J. E., LAHOZ-BELTRA, R., SAMSONOVICH, A. & RASMUSSEN, S. (1992). *IEEE Computer* **25(11)**, 30–39.
HAMEROFF, S. R. & WATT, R. C. (1982). *J. Theor. Biol.* **98**, 549.
HORIO, T. & HOTANI, H. (1986). *Nature* **321**, 605.
HOTANI, H., LAHOZ-BELTRA, R., COMBS, B., HAMEROFF, S. R. & RASMUSSEN, S. (1992). *Nanobiology* **1**, 61–74.
KIM, H., JENSEN, C. G. & REBHUND, L. I. (1986). In: *Dynamic Aspects of Microtubule Biology* (Soifer, D., ed.) *Ann. N.Y. Acad. Sci.* **466**, 218–239.
KIRSCHNER, M. & MITCHISON, T. (1986). *Cell* **45**, 329.
KRETSCHMER, K. & BINDER, K. (1979). *Z. Phys. B.* **34**, 375.
KUDO, T., TADA, K., TAKEDA, M. & NISHIMURA, T. (1990). *Stroke* **21**, 1205–1209.
KWAK, S. & MATUS, A. (1988). *J. Neurocytol.* **17**, 189–195.
LEE, J. C., FIELD, D. J., GEORGE, H. J. & HEAD, J. (1986). *Ann. N.Y. Acad. Sci.* **466**, 111–128.
LYNCH, G. & BAUDRY, M. (1987). *Brain Res. Bull.* **18**, 809–815.
MARGULIS, L., TO, L. & CHASE, D. (1978). *Science* **200**, 1118.
MATSUYAMA, S. S. & JARVIK, L. F. (1989). *Proc. natn. Acad. Sci., U.S.A.* **86**, 8152–8156.
MATTHIAS, B. T. (1973). In: *Proceedings of the Third International Conference "From Theoretical Physics to Biology"*, pp. 12–20. Basel: Karger.
MELKI, R., CARLIER, M. F., PANTALONI, D. & TIMASHEFF, S. N. (1989). *Biochem.* **28**, 9143.
MILEUSNIC, R., ROSE, S. P. & TILLSON, P. (1980). *Neur. Chem.* **34**, 1007–1015.
MITHIEUX, G., CHAUVIN, F., ROUX, B. & ROUSSET, B. (1985). *Biophys. Chem.* **22**, 307–316.
MOSHKOV, D. A., SAVALJEVA, L. N., YANJUSHINA, G. V. and FUNTIKOV, V. A. (1992). *Acta Histochem. Suppl-Band* **XLI(S)**, 241–247.
RASMUSSEN, S., KARAMPURWALA, H., VAIDYANATH, R., JENSEN, K. & HAMEROFF, S. R. (1990). *Physica D* **42**, 428.
REINSCH, S. S., MITCHISON, T. J. & KIRSCHNER, M. (1991). *J. Cell. Biol.* **115(2)**, 365–379.
SABRY, J. H., O'CONNOR, T. P., EVANS, L., TOROIAN-RAYMOND, A., KIRSCHNER, M. & BENTLEY, D. (1991). *J. Cell Biol.* **115(2)**, 831–395.
SILVA, A. J., STEVENS, C. F., TONEGAWA, S. & WANG, Y. (1992). *Science* **257**, 201–206.
SILVA, A. J., PAYLOR, R., WEHNER, J. M. & TONEGAWA, S. (1992). *Science* **257**, 206–211.
STEBBINGS, H. & HUNT, C. (1982). *Cell Tiss. Res.* **227**, 609.
STEIN, D. L. (ed.) (1992). *Spin Glasses and Biology*. Singapore: World Scientific.
SUZUKI, M. (1977). *Prog. Theor. Phys.* **58**, 1151.
SURRIDGE, C. D. & BURNS, R. G. (1992). *Biochemistry* **31**, 6140–6144.
TABONY, J. & JOB, D. (1992). *Proc. natn. Acad. Sci. U.S.A.* **89**, 6948–6952.
TABONY, J. & JOB, D. (1992). *Nanobiology* **1(2)**, 131–147.
THEURKAUF, W. E. & VALLEE, R. B. (1983). *J. Biol. Chem.* **258**, 7883–7886.
WANG, N. & RASENICK, M. M. (1991). *Biochemistry* **30**, 10957–10965.